

View Article Online
View Journal

Journal of Materials Chemistry C

Materials for optical, magnetic and electronic devices

Accepted Manuscript

This article can be cited before page numbers have been issued, to do this please use: S. Gebel, O. Aiboudi, P. Derakhshanfar, J. Shin, U. Langklotz, F. Lissel and U. Kraft, *J. Mater. Chem. C*, 2025, DOI: 10.1039/D5TC01677K.



This is an Accepted Manuscript, which has been through the Royal Society of Chemistry peer review process and has been accepted for publication.

Accepted Manuscripts are published online shortly after acceptance, before technical editing, formatting and proof reading. Using this free service, authors can make their results available to the community, in citable form, before we publish the edited article. We will replace this Accepted Manuscript with the edited and formatted Advance Article as soon as it is available.

You can find more information about Accepted Manuscripts in the <u>Information for Authors</u>.

Please note that technical editing may introduce minor changes to the text and/or graphics, which may alter content. The journal's standard <u>Terms & Conditions</u> and the <u>Ethical guidelines</u> still apply. In no event shall the Royal Society of Chemistry be held responsible for any errors or omissions in this Accepted Manuscript or any consequences arising from the use of any information it contains.



Reversible switching through irradiation of capacitors and organic transistors employing dielectrics blended with non-ionic molecular photoswitches

Sten Gebel¹, Oumaima Aiboudi², Parham Derakhshanfar¹, Jihyun Shin¹, Ulrike Langklotz³, Franziska Lissel^{2,4}, Ulrike Kraft¹

1. Abstract

One promising approach to introduce additional functionalities for sensing and memory applications into conventional organic electronic devices is the introduction of stimuli responsive additives, such as molecular switches. These small organic molecules undergo reversible isomerization between (at least) two isomers when irradiated with light of different wavelength resulting in drastic changes in physicochemical properties such as frontier orbital energy levels, dipole moment and/or molecular geometry. These reversible changes in molecular properties can be exploited to deliberately modify charge transport in organic field-effect transistors and therefore enable optical control over device characteristics.

stimuli-responsiveness organic transistors achieved incorporating the Here, is dihydroazulene/vinylheptafulvene (DHA/VHF) molecular switches into the gate dielectric. To systematically explore this novel approach, we firstly provide a detailed evaluation of the dielectric properties of the DHA/VHF blends with the dielectric polymer poly(methyl methacrylate) in metalinsulator-metal capacitors using impedance spectroscopy. Afterwards, these switchable dielectric blends are employed as gate dielectrics in OFETs, allowing optical control over device characteristics and figures of merit such as field-effect mobility and threshold voltage. Furthermore, optical absorption spectroscopy shows that DHA/VHF molecular switches (unlike the well-known spiropyran/merocyanine photoswitch) exhibit excellent resistance to cycling fatigue when incorporated into insulating PMMA matrices.

¹ Organic Bioelectronics Research Group, Max Planck Institute for Polymer Research, Mainz, Germany

² Leibniz Institute for Polymer Research, Dresden, Germany

³ Fraunhofer Institute for Ceramic Technologies and Systems IKTS, Dresden, Germany

⁴ Hamburg University of Technology, Hamburg, Germany

2. Introduction

Open Access Article. Published on 27 Oktoba 2025. Downloaded on 28/10/2025 19:08:21

The increasing demand for mobile and flexible electronics and the rising interest in the "Internet of Things" promotes research on lightweight organic electronic devices and concepts where the integration of silicon chips is too expensive. Organic field-effect transistors (OFETs) can be used as fundamental building blocks for more advanced electronic circuits and applications on flexible foil and paper substrates 1, such as multi-level photomemories, photodetectors and neuromorphic electronics 2-4.

Here, we give a detailed account of reversible switching of poly(methyl methacrylate) (PMMA) blends with dihydroazulene/vinylheptafulvene (DHA/VHF) photo-/thermochromic molecules. These molecular switches are promising candidates for enabling novel light-responsive organic electronic devices, since they exhibit a large change in dipole moment, but do not contain any ionic which are known to be detrimental for efficient charge carrier transport. For the spiropyran (SP)/merocyanine (MC) switch for example, the zwitterionic merocyanine has been reported to act as scattering site in functionalized transistors⁵⁻⁷. Furthermore, transistors with PMMA:SP/MC gate dielectrics have been reported to be only optically responsive in the bottom-gate configuration, while top-gate transistors are optically inactive due to phase separation, leading to reduced applicability of the system.

So far DHA/VHF switches only received little attention in the context of stimuli-responsive organic devices and previous reports focused mostly on single-molecule junctions or devices based on self-assembled monolayers 8-11. In this work we functionalize PMMA gate dielectrics with DHA/VHF switches to enable light-programmable top-gate organic transistors. The absence of any ionic moieties in both isomers of the DHA/VHF switches allows, to solely study the effect of the change in dipole moment of the switch (~6-10 D for DHA derivative versus ~ 10-15 D for VHF derivatives) on the dielectric properties of PMMA:DHA/VHF capacitors (MIM, metal-insulator-metal devices) and the device performance of organic transistors. (A schematic illustration is depicted in Figure 1.)

The gate dielectric is able to dramatically influence morphology, energetic disorder or trapping at the semiconductor/dielectric interface and therefore charge transport and device performance 12. In this context, the dielectric permittivity ε_r is a key material property. High permittivities for example are generally required for low voltage operation 13-15, but can also induce energetic disorder and hence lower carrier mobilities 16, 17. Impedance spectroscopy is a commonly-used method to study dielectric properties of insulating polymers and several examples can be found in the literature where it was used to study the effect of small molecule additives such as azo dyes or other organic chromophores within a dielectric matrix ¹⁸⁻²⁰. Here, we apply impedance spectroscopy in a different context to investigate the photoisomerization of photochromic molecules (also called photoswitches). Photoswitches are molecules that undergo reversible isomerization between (at least) two isomers due to irradiation with light of different wavelengths. Both isomers can exhibit differences in physicochemical properties such as π -conjugation, molecular geometry and/or dipole moment. When switching from DHA to VHF, the increase in the dipole moment will lead to an increase in permittivity and hence to an increase of the capacitance of PMMA:DHA/VHF blends. When applied as gate dielectrics in transistors an increase in capacitance is expected to be reflected in higher drain currents.

As the dipole moments of the two isomers differs significantly, impedance spectroscopy on PMMA:DHA/VHF MIM capacitors will be a valuable tool to investigate the photoswitching and its effect on the dielectric properties of the insulating matrix. The reversible switching of the overall capacitance due to isomerization of photoswitches has been reported by several groups, e.g. via blending azobenzenebased photoswitches into PMMA ²¹ or via synthesizing spiropyran-containing dielectric copolymers ²². However, detailed characterizations of impedance data, frequency-dependence and how the lightinduced isomerization of photoswitches e.g. affects dielectric permittivity ε_r and dielectric loss ε_r " of lightresponsive insulating blends are scarce 23. These kinds of data could not only give further insights into underlying mechanisms, but also allow to quantify the switching capability of photochromic molecules. In this study, it is shown that the stimulus-induced isomerization of the dihydroazulene/vinylheptafulvene (DHA/VHF) photoswitches within a PMMA matrix can be directly observed by measuring the frequencydependent complex electrical impedance Z*. From the impedance spectra the switching parameters such as the complex dielectric permittivity ε_r^* and the area-normalized capacitance of the gate dielectric are derived. An alternative approach to analyzing impedance data is the fitting with an equivalent circuit. This method is widely used in many fields such as electroceramics ²⁴, battery research ²⁵ or biosensing ²⁶. However, to the best of our knowledge there is no systematic study implementing and assessing an equivalent circuit model for light switchable organic capacitor devices. Here, an equivalent circuit fitting methodology is employed serving as alternate approach to evaluate the switching capabilities of the DHA/VHF molecules in functioning electronic devices. Furthermore, it is demonstrated for the first time that PMMA:DHA/VHF blend gate dielectrics in organic transistors enable the control of transistor characteristics and figures of merit, by applying external stimuli such as UV light and heat. Additionally, it is shown that DHA/VHF molecular switches (unlike the established SP/MC photoswitch) exhibit excellent resistance to cycling fatigue when incorporated into a PMMA dielectric.

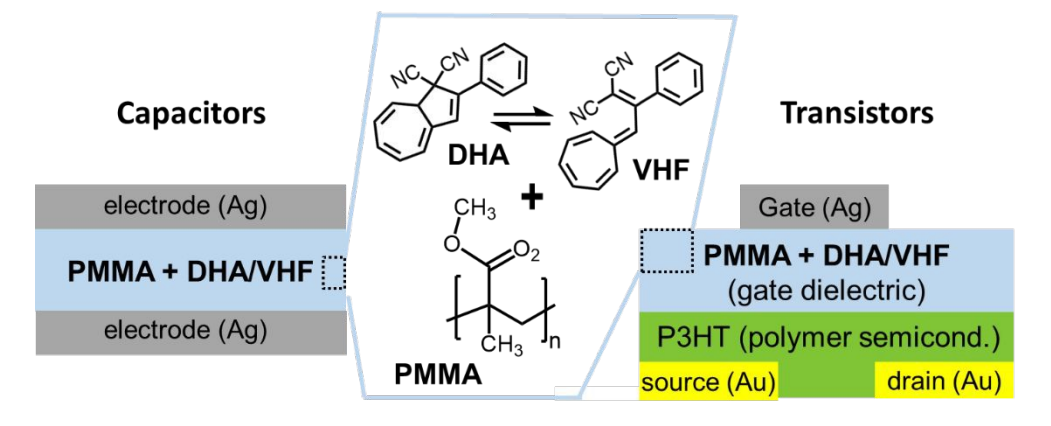


Figure 1: Schematic illustration of capacitors (MIM, metal-insulator-metal devices) and bottom-contact top-gate polymer transistors with gate dielectrics based on PMMA blends with DHA/VHF photo-/thermochromic molecules and the molecular structures of PMMA, DHA and VHF.

3. Experimental Details

Materials and solution preparation

The molecular switches DHA-Ph, DHA-OMe and DHA-F₂ were synthesized as previously described ²⁷ (see Error! Reference source not found. for molecular structure of the photoisomers for the three photoswitches). PMMA (product number 200336, average molecular weight = 15 kDa, PDI: 1.83) and regioregular P3HT (poly(3-hexylthiophen, product number 445703, molecular weight = ~50 kDa, regioregularity > 90 %, further information is provided in the ESI, section 9) were purchased from Sigma Aldrich and used without further purification. PMMA stock solutions were prepared with anhydrous trichloromethane (80 mg/mL, for capacitor and UV/Vis absorption spectroscopy experiments) or anhydrous ethyl acetate (120 mg/mL, for transistor experiments). For the photoswitch stock solutions, the solvent was chosen to match the solvent of PMMA (35 to 40 mg/mL in anhydrous trichloromethane or 52 to 60 mg/mL in anhydrous ethyl acetate). PMMA and switch solutions were prepared in air and stirred over night at room temperature, while P3HT solutions (10 mg/mL in anhydrous chlorobenzene) were prepared in a nitrogen-filled glovebox and stirred over night at 60 °C. The final PMMA solutions (40 mg/mL in anhydrous trichloromethane or 60 mg/mL (80 mg/mL for PMMA-only reference) in anhydrous ethyl acetate) were prepared by adding either switch stock solution or additional solvent (for reference devices) to the PMMA stock solution and were stirred for 2 h at room temperature prior to spin coating. The molar fractions of photoswitch (with respect to a single PMMA repeat unit) in these solutions was 14.6 mol% (i.e. 14.6 switch molecules in proportion to 100 PMMA repeat units), resulting in the following mass fractions: 30.44 wt% (DHA-Ph), 32.89 wt% (DHA-OMe) and 33.33 wt% (DHA-F₂).

3.2. <u>Device fabrication and UV/Temperature treatments</u>

Capacitors (metal-insulator-metal structures ²⁸) and bottom-contact/top-gate transistors were fabricated on glass substrates. Prior to bottom electrode deposition, the substrates were cleaned via sonicating in ultrapure water (5 min), acetone and isopropanol (both 10 min). After drying the substrates in an oven (10 min at 140 °C) a UV/ozone treatment was applied for 20 min. Capacitor bottom electrodes (5 nm chromium/100 nm silver) and transistor source and drain electrodes (2 nm chromium/30 nm gold, channel length = 30 μ m, channel width = 1 mm) were thermally evaporated in vacuum (< 1x10⁻⁷ mbar) through shadow masks. The glass substrates for transistors were exposed to 20 min UV/ozone treatment prior to deposition of the organic semiconductor layer. P3HT films (thickness = 30-35 nm) were fabricated via spin coating at 1500 rpm for 30 s and annealed for 30 min at 150 °C. PMMA:photoswitch blends or bare PMMA dielectrics were spin coated either on top of the bottom electrode (capacitors) or the P3HT film (OFETs) at 2000 rpm for 60 s to yield films with a thickness of 600-650 nm/ 710-730 nm (trichloromethane/ethyl acetate) for films containing PMMA:photswitch blends and 400-460 nm/ 700-720 nm (trichloromethane/ethyl acetate) for bare PMMA films. (Thickness profiles are shown in Figure S22 in the ESI.) All PMMA films were annealed for 20 min at 90 °C. Finally, 20 nm of silver were evaporated through shadow masks onto the dielectric as semi-transparent top electrodes. (For the capacitors, the area of electrode overlap A is 1 mm².) All thin-film samples and devices were illuminated using a Dymax ECE 2000 flood lamp (13 mW/cm² at 320 to 390 nm) and the dose was monitored using a Dymax Accu-Cal 50 UV dose meter. A fixed UV dose (as measured by the dose meter) of 5 J/cm² was applied in all experiments. Thermal switching (from VHF to DHA) was carried out on a hot plate at 90 °C for 5 min. If not indicated otherwise all fabrication steps from deposition of the bottom electrodes to characterization and illumination/annealing were carried out in a nitrogen-filled glovebox.

3.3. Transistor characterization

The polymer transistors were characterized in the dark, in a nitrogen-filled glovebox using a Keithley 4200-SCS parameter analyzer. Transistor figures of merit, i.e. field-effect mobility and threshold voltage were derived from transfer characteristics following procedures described in the literature 29 . The V_{GS} fitting range for determining the threshold voltage was chosen from -20 to -50 V. Constant bias stress was applied for 2 h (cumulative) between drain and source electrodes (V_{DS} = -50 V) and gate and source electrodes (V_{GS} = -50 V) 30 . During this time the bias stress was only paused to record transfer characteristics.

3.4. Impedance spectroscopy and impedance data analysis

Impedance spectra were recorded in the dark under ambient conditions using a Novocontrol Alpha-A impedance analyzer with a ZG4 test interface and measurements were carried out in air by applying an AC voltage of 1 V rms and sweeping the angular frequency from 10⁶ to 1 Hz (35 data points with equal logarithmic spacing, no DC off-set). EISSA (Electrochemical Impedance Spectroscopy Spectrum Analyzer) software was used for fitting of the impedance data. The details of the fitting procedure, equations and further information on the impedance formalism that was adapted in this study can be found in the Supporting Information (section 3).

4. Results and Discussion

4.1. Photo switchable capacitors

Three different derivatives of DHA/VHF molecular switches were blended with PMMA in order to fabricate light switchable capacitors (MIM, metal-insulator-metal devices). Error! Reference source not found. shows the molecular structures of the switches, namely DHA/VHF-Ph, DHA/VHF-OMe and DHA/VHF-F₂. Ionization potentials, electron affinities and dipole moments of these materials are summarized in Error! Reference source not found. The isomerization from DHA to VHF was induced by exposure to UV light, while the backreaction from VHF to DHA was achieved via thermal annealing at 90 °C for 5 min. Figure 2a clearly depicts the typical color change from pale yellow (DHA) to orange/red (VHF), indicating that the isomerization reaction readily occurs in the PMMA matrix. For the capacitor and transistor devices 20 nm of silver were used as semi-transparent top electrodes, allowing for high UV light transparency (see Error! Reference source not found.). This switching is also evident in the obtained impedance data: In order to study the switching of the DHA/VHF molecules in the PMMA matrix, capacitors were subjected to eight switching cycles, where one cycle consists of a UV exposure step (DHA to VHF) and one thermal annealing step (VHF to DHA). After each UV and each annealing step, the impedance spectrum was measured. Figure **2b-d** depicts the data as Nyquist plot (Z" vs. Z') as well as Bode plot ($|Z^*|$ vs. f and phase angle φ vs. f) for eight cycles of switching for a PMMA:DHA/VHF-Ph blend capacitor. The corresponding data for PMMA:DHA/VHF-OMe blend, PMMA:DHA/VHF-F₂ blend and a reference capacitor without any photoswitch can be found in Error! Reference source not found.

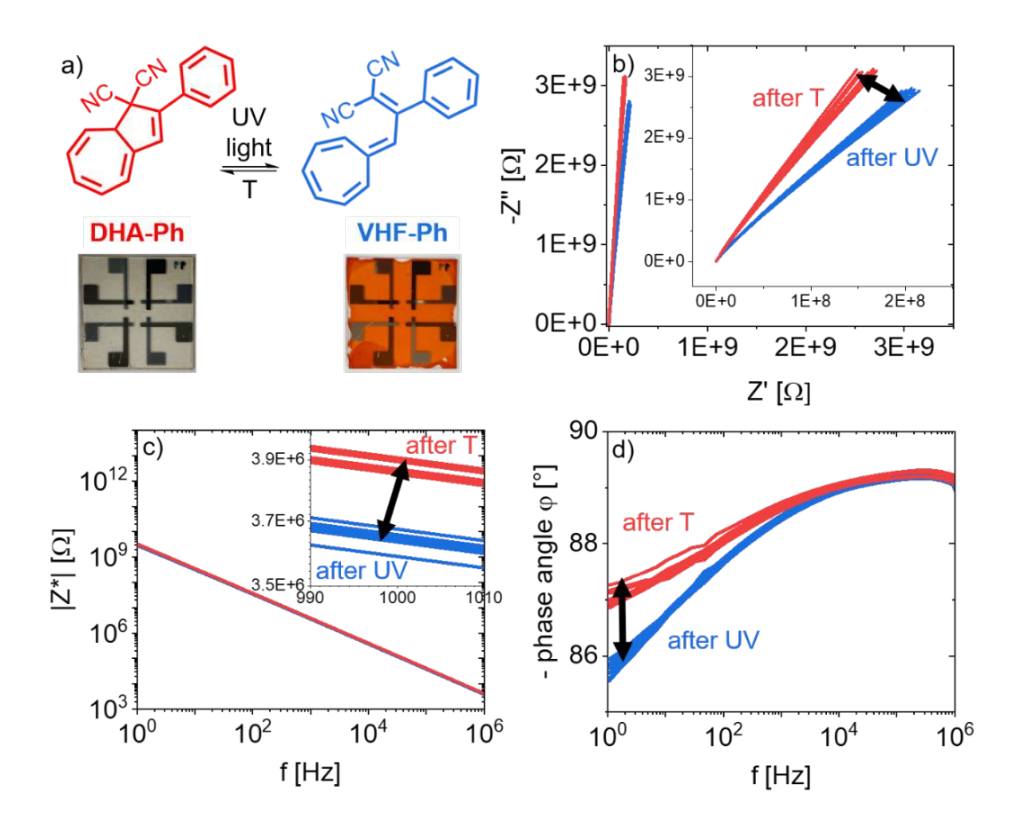


Figure 2: Stimuli-responsive capacitors enabled by PMMA blends with DHA/VHF-Ph photo-/thermochromic molecules. a) Molecular structure of both isomers of the molecular switch and photographs of a substrate with four capacitor devices after thermal annealing (left, switch in DHA form) and after UV light exposure (right, switch in VHF form). b) - d) Nyquist and Bode plot of impedance data collected for eight switching cycles. Traces in red correspond to data measured after annealing and traces in blue correspond to data measured after UV exposure. (The Nyquist plot in panel b) is shown on orthonormal axes, while its inset is not. Note that phase angles of capacitors are negative per definition, which describes the scenario that the current is leading the voltage.)

Based on these data, the frequency-dependent complex dielectric permittivity ε_r^* was evaluated by calculating its real part ε_r' and imaginary part ε_r'' (for every frequency) using Equations 1 to 3, with the thickness of the dielectric d, vacuum permittivity ε_0 and area of electrode overlap A (= 1 mm²). ε_r' and ε_r'' are sometimes referred to as dielectric permittivity and dielectric loss respectively ²³. Further information on this impedance formalism is given in the Electronic Supplementary Information, ESI (section 3).

$$\varepsilon_{r}' = \frac{d}{\omega \varepsilon_0 A} \cdot \frac{-Z''}{(Z'^2 + Z''^2)} \tag{1}$$

$$\varepsilon_r^{"} = \frac{d}{\omega \varepsilon_0 A} \cdot \frac{Z^{\prime}}{(Z^{\prime 2} + Z^{\prime \prime 2})} \tag{2}$$

$$|\varepsilon_r^*| = \sqrt{\varepsilon_r'^2 + \varepsilon_r''^2} \tag{3}$$

Figure 3a,b show that both, the real and imaginary part of the permittivity increase after UV exposure. The increase in the imaginary part is more pronounced at lower frequencies. Furthermore, the modulus of the complex permittivity $|\varepsilon_r^*|$ and the loss tangent $tan(\delta)$ were calculated (see Error! Reference source **not found.**). In absolute values, $|\varepsilon_r^*|$ switches between around 3.56 and 3.96 (at f = 1 Hz), which corresponds to a switching of capacitance (per unit area) between 4.9 and 5.4 nF/cm². The frequencyindependent increase in ε_r upon UV irradiation is related to the increased dipole moment of VHF in comparison to DHA (see Error! Reference source not found.) resulting in a larger polarizability of the blend. Furthermore, Figure 2 indicates a slight decrease in resistance after UV irradiation, which is consistent with an increase in dielectric loss and in agreement with increased single molecule conductance of VHF correlated with the reduced HOMO-LUMO gap 8,31 . The switching in ε_r " at low frequencies could also stem from switch molecules affecting the relaxation of the PMMA side groups. It has been reported that the relaxation of the carboxymethyl (-COOCH₃) side groups (β relaxation mode) results in a peak in the ε_r " spectrum between 1 and 10 Hz ¹⁸, which is in good agreement with our results (see **Error!** Reference source not found.). However, in the blend system with DHA/VHF this relaxation peak cannot be observed, possibly due to the fact that the presence of the switches hinders the movement of the polymer side groups, with this effect being stronger for DHA compared to VHF. Our results show that the contribution of $\varepsilon_{r'}$ (related to the changing dipole moment of DHA/VHF) dominates the strong increase in $|\varepsilon_r^*|$ (and therefore capacitance) after UV illumination. Similar results were reported for PMMA-based capacitors containing azobenzene ²¹ and spiropyran ²². **Figure 3c,d** show the relative changes of $|\varepsilon_r^*|$ (from one processing step to the next) as a function of frequency and after each individual step. These results indicate that the modulus of the permittivity increases as a result of UV exposure (consistent with the increasing dipole moment, see Error! Reference source not found. 32), while it decreases after thermal annealing. Furthermore, the changes are more pronounced at lower frequencies (due to the contribution of ε_r ") and no apparent cycling fatigue (reduction in magnitude of switching) can be observed.

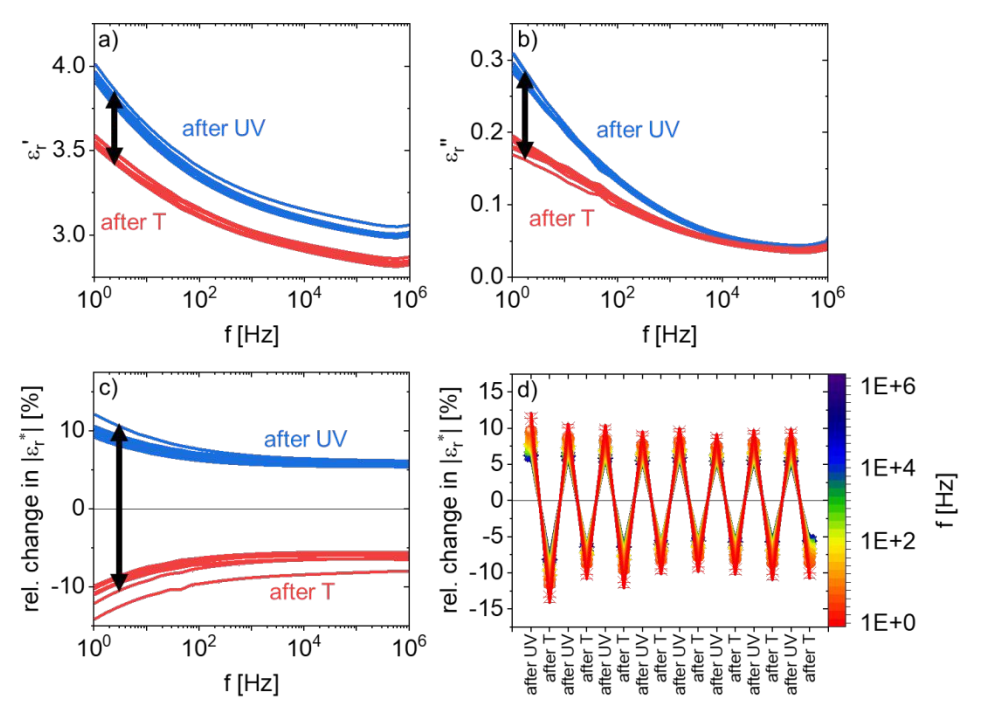


Figure 3: Analysis of the frequency-dependent complex permittivity ε_r^* . a) – b) Real and imaginary part of ε_r^* . c) Relative change in the modulus of the complex permittivity (from one processing step to the next) as a function of frequency. Traces in red correspond to data measured after annealing and traces in blue correspond to data measured after UV exposure. d) Relative change in the modulus of the complex permittivity over the course of eight switching cycles. The color coding from red to dark blue corresponds to the frequency at which the permittivity was evaluated. (Note that panels c) and d) represent the same data in two different ways.)

An alternative approach for evaluating impedance spectra is to fit the data to an equivalent circuit model in order to better understand the physical and chemical processes, which are possibly occurring during the experiment. For example, Rampi et al. reported that alkanethiol self-assembled monolayers between two opposing mercury surfaces can be modelled with an RC element (i.e. resistor and capacitor in parallel) ³³. Jin et al. used a more complicated circuit of a resistor in series with two RC elements to describe the electrochemical processes in electrochromic displays ³⁴. The molecules reported in that study contain photochromic diarylethene units, but their ability to photoisomerize was not investigated with impedance spectroscopy. To the best of our knowledge, there are no reports in the literature, which describe and quantify the switching of photochromic molecules using equivalent circuit analysis. We here employ such a procedure, which in particular allows to extract dielectric permittivities from the frequency-dependent impedance data. The details are given in the Electronic Supplementary Information.

Here, an RC element model is chosen yielding the fitted resistance R and the fitted capacitance C (which can be converted to the area-normalized capacitance C_i). A representative fit of data measured on

PMMA:DHA/VHF-Ph-based MIM devices is given in Figure 4c. (Results obtained with different equivalent circuit models as well as details on the fitting procedure are given in the ESI.) Figure 4a,b show that both circuit parameters of the RC model switch reversibly over the course of eight UV/T cycles. With the fitted capacitance it is possible to calculate the permittivity ε_r of the sample using Equation 4. Furthermore, we conclude that approach of describing the sample as a capacitor is an approximation justified by the large values of resistance (in the $G\Omega$ range).

$$\varepsilon_r = \frac{C_{fitted} \cdot d}{\varepsilon_0 \cdot A} \tag{4}$$

Furthermore, a comparison of the permittivities derived from the RC element model with the results obtained by directly analyzing the complex impedance data (at f = 1 Hz) shows that both approaches yield comparable results (see Figure 4d), underlining the validity of the fitting approach.

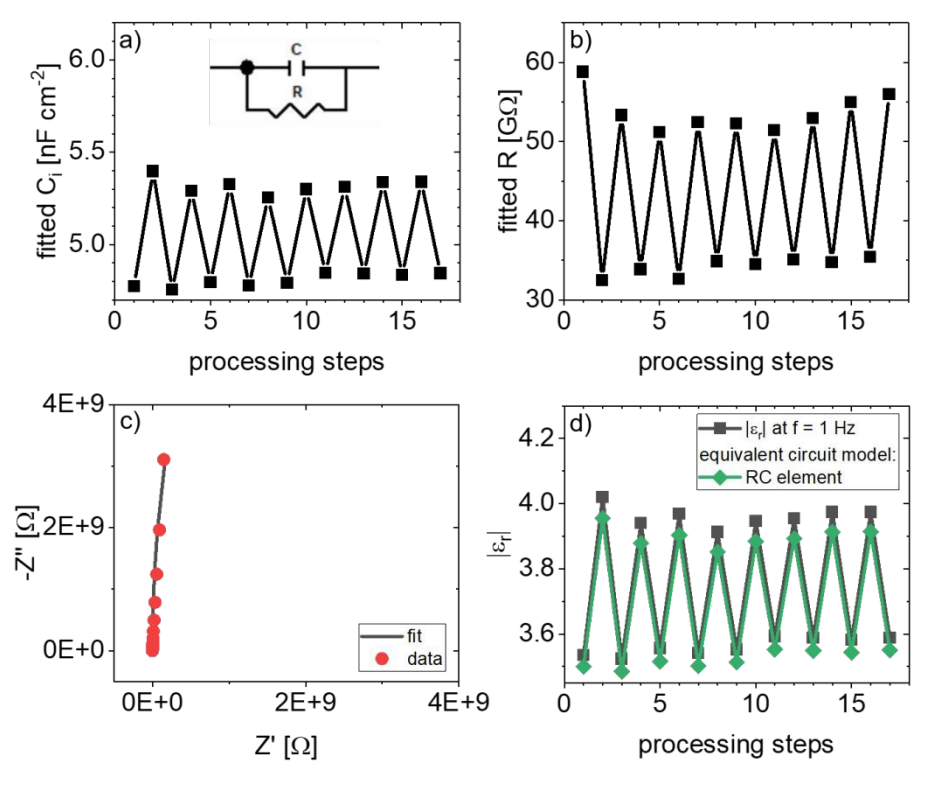


Figure 4: Equivalent circuit fitting analysis using an RC element model of impedance data from a PMMA:DHA/VHF-Ph MIM devices acquired over the course of eight UV/T cycles. Fitted circuit element parameters: a) Area-normalized capacitance, b) resistance. c) Fitted (representative) Nyquist plot on orthonormal axes. d) Resulting permittivities from the equivalent circuit (green diamonds) compared to permittivities from the complex frequency-dependent impedance at f = 1 Hz.

Figure shows the switching in permittivity for PMMA blends containing three different DHA/VHF derivatives obtained via fitting with a RC element model. The largest change in permittivity is observed for blends with the unsubstituted derivative DHA/VHF-Ph, while the lowest change is observed for the fluorinated derivative DHA/VHF-F₂. This trend is in agreement with the expectation based on the calculated dipole moments of the switches (see Error! Reference source not found.). The differences in dipole moment of the isomers were determined as 4.95 D for DHA/VHF-Ph, 4.42 D for DHA/VHF-OMe and 4.22 D for DHA/VHF-F₂. Error! Reference source not found. indicates that the same qualitative trend is obtained when other equivalent circuit models are used. All isomers demonstrate a very good switching stability over multiple cycles.

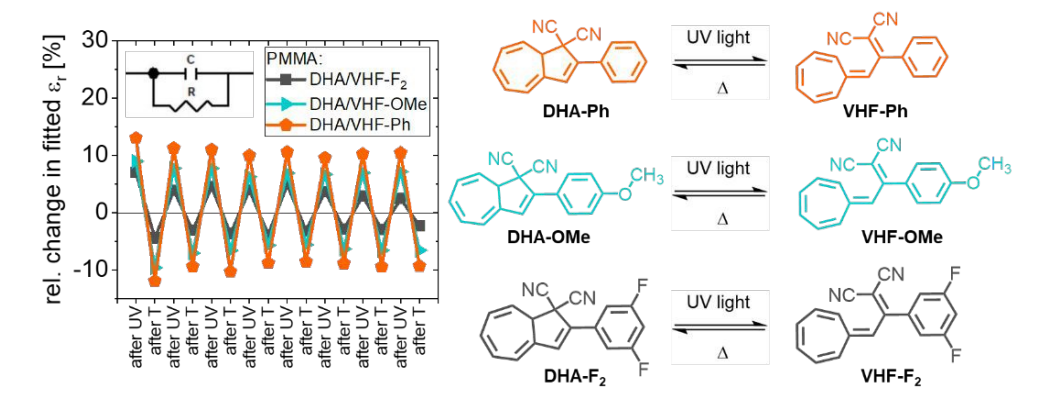


Figure 5: Comparing the switching in permittivity for PMMA:DHA/VHF capacitors containing three different DHA/VHF derivatives (DHA/VHF-Ph, DHA/VHF-OMe, DHA/VHF-F₂). The relative change in permittivity was determined by fitting an RC element model to impedance data collected over the course of eight UV/T cycles.

4.2. UV/Vis absorption

To study the cycling fatigue, PMMA blends with DHA/VHF switches were investigated using UV/Vis absorption spectroscopy. Spectra were recorded on pristine films and after the first UV light irradiation in order to determine the characteristic absorption bands of the DHA and VHF isomers. In agreement with the literature 35 the DHA isomers showed a maximum absorption around 360 to 370 nm, while the VHF isomers absorbed around 470 to 485 nm. Additionally, the switching fatigue of the blend films was studied over the course of 20 UV/T cycles (i.e. 20 UV and 20 annealing steps). All recorded spectra are shown in **Figure 6a** and **Error! Reference source not found.**. The absorbance of the VHF isomer at λ_{max} was used as an indicator of switching fatigue (see ESI for experimental details). **Figure 6b** demonstrates that DHA/VHF-OMe shows remarkable switching stability. After 20 UV/T cycles the VHF absorption has only decreased

by 35 %. Furthermore, all three DHA/VHF derivatives and especially DHA/VHF-OMe show superior fatigue resistance compared to the well-known spiropyran switch, which degrades almost completely within the first 10 cycles. Possibly, the DHA/VHF switches are less prone to photo-oxidation, since they exhibit higher ionization potentials than SP/MC switches (see Error! Reference source not found.). Such photo-oxidation can occur as a result of the repeated UV light exposure and is known to be a major degradation path in spiropyran systems ^{36, 37}. Other reports indicate that spiropyrans tend to aggregate due to the presence of ionic moieties in the merocyanine form ³⁸⁻⁴⁰. Neither DHA nor VHF isomers contain ionic moieties, which presumably is another reason for the improved fatigue resistance.

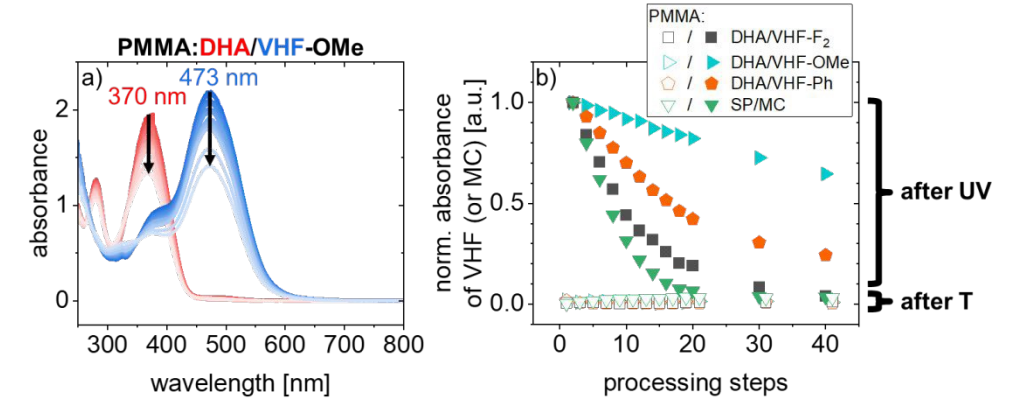


Figure 6: a) UV/Vis absorption spectra of a) PMMA:DHA/VHF-OMe blend films measured over 20 UV/T cycles. Blue traces: Measured after UV light exposure (5 J/cm²). Red traces: Measured after thermal annealing (90 °C for 5 min). b) Comparing cycling fatigue behavior of PMMA:DHA/VHF-OMe, PMMA:DHA/VHF-Ph, PMMA:DHA/VHF-F₂ and PMMA:SP/MC (spiropyran/ merocyanine) blend films using UV/Vis absorption spectroscopy. The graph displays the normalized absorption (measured at wavelength of maximum absorption) of VHF around 470 to 480 nm and MC around 570 nm (respectively). Empty symbols indicate that the switch is in its DHA (or SP) form.

4.3. Photoswitchable transistors

The first successful application of insulating polymer:photoswitch blends as gate dielectrics in OFETs was reported by Shen et al. 41. The authors blended spiropyran molecules into PMMA and observed an increase in capacitance due to photoisomerization of the low dipole moment spiropyran to the high dipole moment merocyanine. Increased drain current in transistors was ascribed to the increase in dielectric permittivity. Lee et al. used blends of PMMA and azobenzene switches to construct UV sensors and also concluded that isomerization to the high dipole moment isomer of the photoswitch increases the capacitance of the dielectric blend which in turn leads to higher drain current in transistors 42. Here, this concept of light-switchable gate dielectrics is extended for the first time to blends with DHA/VHF molecular switches. PMMA:DHA/VHF blends were applied as gate dielectrics in P3HT OFETs and device This article is licensed under a Creative Commons Attribution 3.0 Unported Licence.

Open Access Article. Published on 27 Oktoba 2025. Downloaded on 28/10/2025 19:08:21

characteristics were recorded over the course of eight UV/T cycles. The resulting transfer and output characteristics for transistors with PMMA:DHA/VHF blend and unblended PMMA (as reference) dielectrics are summarized in Figure 7, Error! Reference source not found. and Error! Reference source not found.. Figure 7a shows that the obtained transfer characteristics for transistors with PMMA:DHA/VHF-OMe blend dielectric after UV and after thermal annealing can be clearly distinguished. In contrast to previous reports employing PMMA:SP/MC blends 43, 44, these characteristics show only negligible hysteresis regardless of the state of the switch. UV exposure leads to an increase in drain current caused by a shift of the threshold voltage (of around 15 V) towards more positive gate-source bias. Furthermore, the modulation of the transfer characteristics can be related to a change in field-effect mobility as indicated in Figure7b. Similar behavior was observed for the blends with DHA/VHF-Ph and DHA/VHF-F₂ (see Error! Reference source not found.). A quantitative comparison of the stimuli-modulated field-effect mobility (determined at maximum negative gate bias) for blends with three different derivatives of the switch is given in Figure 7c. The area-normalized capacitances of the gate dielectrics that were used to calculate the mobilities, are summarized in Error! Reference source not found.. These values were calculated by using the dielectric permittivities obtained by fitting impedance data using a single capacitor as equivalent circuit (see ESI for details). The reversible shifts of threshold voltage for all three blends are shown in Error! Reference source not found. as well as further characterization including bias stress (Figure \$19) and long-term (Figure S20) stability.

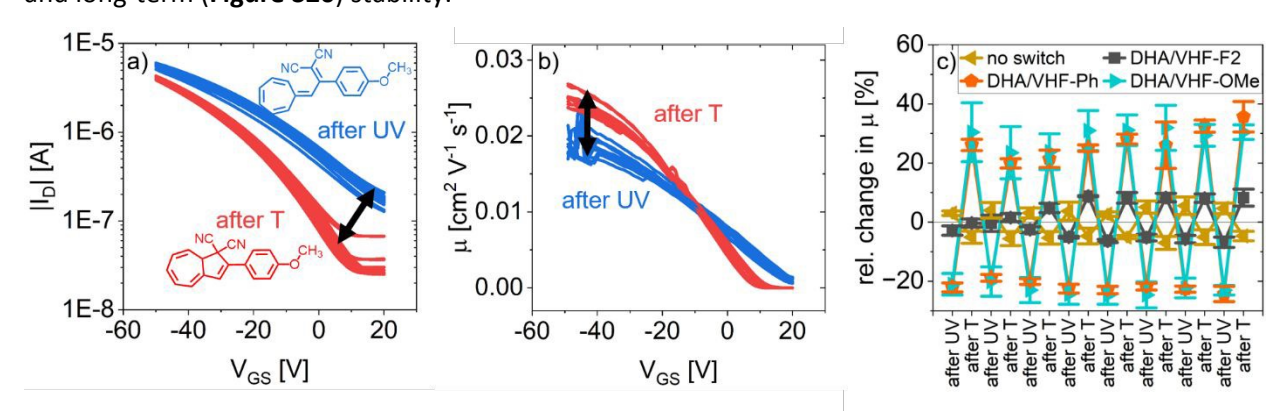


Figure 7: Stimuli-responsive organic transistors enabled by using PMMA blends with DHA/VHF photo-/thermochromic molecules as gate dielectrics. a) Reversible changes of transfer characteristics in a transistor with PMMA:DHA/VHF-OMe dielectric induced by UV light illumination (blue lines) and thermal annealing (red lines) for eight UV/T cycles ($V_{DS} = -50$ V). b) Gate-source bias-dependent field-effect mobilities. c) Reversible change in mobility (at $V_{GS} = -50 \text{ V}$) for blends containing three different DHA/VHF derivatives (PMMA:DHA/VHF-OMe, PMMA:DHA/VHF-Ph, PMMA:DHA/VHF-F2) and a reference device without any switch. (The error bars represent the standard deviation of at least three devices.)

urnal of Materials Chemistry C Accepted Manuscrip

In our previous work we were able to show that stimuli-responsive organic transistors can be enabled by blending DHA/VHF molecular switches into the active channel (semiconductor) of the device 32. A reversible tuning of transfer characteristics was observed upon alternating UV light irradiation and thermal annealing. Increased on-current and a shift of threshold voltage towards more positive gatesource bias as a consequence of UV irradiation suggested that the VHF isomer can act as a dopant, which is activated with light. Here, we report similar observations, when incorporating DHA/VHF photoswitches into the gate dielectric, rather than the active layer. Due to the spatial separation of the switch and the semiconductor, it seems unlikely that a doping-like mechanism can occur. Hence, other effects such as a change in gate dielectric capacitance (which was observed experimentally, see above) or energetic disorder should be considered. As discussed in the previous section, the isomerization from DHA to VHF increases the dielectric permittivity of PMMA:DHA/VHF blends and therefore yields an increase of the capacitance of the gate dielectric of the transistor. This should be expected to lead to higher drain currents, but should either not affect the threshold voltage or rather lead to more negative threshold voltages 45. Veres et al. reported that energetic disorder at the semiconductor-dielectric interface induced by large molecular dipoles within the dielectric leads to lower mobility and shifts the threshold voltage to more negative gate-source bias ¹⁶. In our case, a transition from the low dipole moment DHA to the high dipole moment VHF leads to a decrease in mobility and a threshold voltage shift to more positive gatesource bias. Therefore, the changing capacitance and the energetic disorder both fail to fully explain our results and a more complicated mechanism or two effects simultaneously seem to be at place. Potential explanations include 1) interfacial mixing between the PMMA:photoswitch blend and the semiconductor and/or 2) phase separation between PMMA and the photoswitch which brings the latter in direct contact with the semiconductor. Both scenarios could potentially cause doping effects through the strong electron accepting properties of VHF 46, similar to when the switch is blended directly into the semiconductor. Alternatively, the formation of photoswitch aggregates with at least partially aligned dipole moments and the resulting built-in electric field would also cause threshold voltage shifts towards more positive threshold voltages, as observed for OFETs employing well-ordered SAM-based interfacial dipoles 14, 47-49. In order to clarify the exact mechanism at place, further experimental studies carefully examining the microstructure of the interface will be necessary.

5. Conclusion

In the first part of this study, capacitors were fabricated by blending the insulating polymer PMMA with DHA/VHF photo-/thermochromic molecules. The reversible isomerization of the molecular switches can be observed in capacitors (MIM, metal-insulator-metal devices) and is studied in detail by using impedance spectroscopy. In order to quantify the reversible switching of the system, the resulting impedance data is analyzed by following two different approaches: 1) Calculating the frequency-dependent complex dielectric permittivity from the real and the imaginary part of the complex impedance for every frequency and 2) Determination of the dielectric permittivity through equivalent circuit fitting of the complex impedance data. To the best of our knowledge, this is the first time that an equivalent circuit fitting methodology is applied to investigate the photoisomerization of molecular switches. In addition to the switching of the capacitance/permittivity, the fit of an RC-element captures a slight switching of a resistive component which correlates well with previous reports on switching of single molecule conductance. This study underlines that impedance spectroscopy is a straightforward tool to capture and accurately quantify the reversible switching of photochromic molecules in stimuli-responsive organic electronic devices.

Furthermore, the PMMA:DHA/VHF blends are successfully applied to construct light- and temperature-responsive organic transistors. We show that the transistor characteristics can be tuned reversibly via the isomerization of DHA/VHF molecular switches within the gate dielectric. The charge carrier mobility in particular is modulated by around 20 - 30 % by applying subsequent UV light and thermal annealing treatments. Finally, the superior resistance to switching fatigue compared to the known spiropyran switch is demonstrated. It can be concluded that DHA/VHF molecular switches and the reported reversibly switchable transistors open up new opportunities for next-generation stimuli-responsive organic electronic devices and memory applications.

6. Acknowledgements

The authors thank C. Bauer, M. Beuchel, F. Keller, S. Koynova and V. Maus for the technical support. This work was partially funded by the German Research Foundation (DFG) under Grant 551494522. FL thanks the Ingeborg-Gross foundation.

7. References

This article is licensed under a Creative Commons Attribution 3.0 Unported Licence.

Open Access Article. Published on 27 Oktoba 2025. Downloaded on 28/10/2025 19:08:21

- 1. U. Kraft, T. Zaki, F. Letzkus, J. N. Burghartz, E. Weber, B. Murmann and H. Klauk, *Advanced Electronic Materials*, 2019, **5**, 1800453.
- 2. S. Lee, S. Kim and H. Yoo, *Polymers*, 2021, **13**, 3774.
- 3. Y. Wakayama, R. Hayakawa and H.-S. Seo, *Science and Technology of Advanced Materials*, 2014, **15**, 024202.
- 4. J. Milvich, T. Zaki, M. Aghamohammadi, R. Rödel, U. Kraft, H. Klauk and J. N. Burghartz, *Organic Electronics*, 2015, **20**, 63-68.
- 5. Y. Ishiguro, R. Hayakawa, T. Chikyow and Y. Wakayama, *Journal of Materials Chemistry C*, 2013, **1**, 3012-3016.
- 6. Y. Ishiguro, R. Hayakawa, T. Yasuda, T. Chikyow and Y. Wakayama, *ACS Applied Materials & Interfaces*, 2013, **5**, 9726-9731.
- 7. Y. Ishiguro, R. Hayakawa, T. Chikyow and Y. Wakayama, *ACS Applied Materials & Interfaces*, 2014, **6**, 10415-10420.
- 8. S. Lara-Avila, A. V. Danilov, S. E. Kubatkin, S. L. Broman, C. R. Parker and M. B. Nielsen, *The Journal of Physical Chemistry C*, 2011, **115**, 18372-18377.
- 9. S. L. Broman, S. Lara-Avila, C. L. Thisted, A. D. Bond, S. Kubatkin, A. Danilov and M. B. Nielsen, *Advanced Functional Materials*, 2012, **22**, 4249-4258.
- 10. C. Huang, M. Jevric, A. Borges, S. T. Olsen, J. M. Hamill, J.-T. Zheng, Y. Yang, A. Rudnev, M. Baghernejad, P. Broekmann, A. U. Petersen, T. Wandlowski, K. V. Mikkelsen, G. C. Solomon, M. Brøndsted Nielsen and W. Hong, *Nature Communications*, 2017, **8**, 15436.
- 11. T. Li, M. Jevric, J. R. Hauptmann, R. Hviid, Z. Wei, R. Wang, N. E. A. Reeler, E. Thyrhaug, S. Petersen, J. A. S. Meyer, N. Bovet, T. Vosch, J. Nygård, X. Qiu, W. Hu, Y. Liu, G. C. Solomon, H. G. Kjaergaard, T. Bjørnholm, M. B. Nielsen, B. W. Laursen and K. Nørgaard, *Advanced Materials*, 2013, **25**, 4164-4170.
- 12. Y. Wang, X. Huang, T. Li, L. Li, X. Guo and P. Jiang, Chemistry of Materials, 2019, 31, 2212-2240.
- 13. R. P. Ortiz, A. Facchetti and T. J. Marks, *Chemical Reviews*, 2010, **110**, 205-239.
- 14. U. Kraft, U. Zschieschang, F. Ante, D. Kälblein, C. Kamella, K. Amsharov, M. Jansen, K. Kern, E. Weber and H. Klauk, *Journal of Materials Chemistry*, 2010, **20**, 6416-6418.
- 15. U. Kraft, M. Sejfić, M. J. Kang, K. Takimiya, T. Zaki, F. Letzkus, J. N. Burghartz, E. Weber and H. Klauk, *Advanced Materials*, 2015, **27**, 207-214.
- 16. J. Veres, S. D. Ogier, S. W. Leeming, D. C. Cupertino and S. Mohialdin Khaffaf, *Advanced Functional Materials*, 2003, **13**, 199-204.
- 17. T. Richards, M. Bird and H. Sirringhaus, *The Journal of Chemical Physics*, 2008, **128**, 234905.
- 18. I. M. Kalogeras, E. R. Neagu and A. Vassilikou-Dova, *Macromolecules*, 2004, **37**, 1042-1053.
- 19. W. Shi, C. Fang, Q. Pan, X. Sun, Q. Gu, D. Xu and J. Yu, *Reactive and Functional Polymers*, 2000, **44**, 177-182.
- 20. D. Lei, J. Runt, A. Safari and R. E. Newnham, *Macromolecules*, 1987, **20**, 1797-1801.

- 21. V. Zaporojtchenko, C. Pakula, S. W. Basuki, T. Strunskus, D. Zargarani, R. Herges and F. Faupel, *Applied Physics A*, 2011, **102**, 421-427.
- 22. M. Gagliardi, F. Pignatelli and V. Mattoli, Sensors and Actuators A: Physical, 2020, 302, 111804.
- 23. D. Luo and L. Deng, *Applied Physics Letters*, 2006, **88**, 181104.
- 24. J. T. S. Irvine, D. C. Sinclair and A. R. West, Advanced Materials, 1990, 2, 132-138.
- 25. R. R. Gaddam, L. Katzenmeier, X. Lamprecht and A. S. Bandarenka, *Physical Chemistry Chemical Physics*, 2021, **23**, 12926-12944.
- 26. E. P. Randviir and C. E. Banks, *Analytical Methods*, 2022, **14**, 4602-4624.
- 27. K. H. Au-Yeung, T. Kühne, O. Aiboudi, S. Sarkar, O. Guskova, D. A. Ryndyk, T. Heine, F. Lissel and F. Moresco, *Nanoscale Advances*, 2022, **4**, 4351-4357.
- 28. U. Kraft, M. Nikolka, G. J. N. Wang, Y. Kim, R. Pfattner, M. Alsufyani, I. McCulloch, B. Murmann and Z. Bao, *Journal of Physics: Materials*, 2023, **6**, 025001.
- 29. Z. A. Lamport, H. F. Haneef, S. Anand, M. Waldrip and O. D. Jurchescu, *Journal of Applied Physics*, 2018, **124**, 071101.
- 30. M. Nguyen, U. Kraft, W. L. Tan, I. Dobryden, K. Broch, W. Zhang, H.-I. Un, D. Simatos, D. Venkateshavaran, I. McCulloch, P. M. Claesson, C. R. McNeill and H. Sirringhaus, *Advanced Materials*, 2023, **35**, 2205377.
- 31. S. L. Broman and M. B. Nielsen, *Physical Chemistry Chemical Physics*, 2014, **16**, 21172-21182.
- 32. S. Gebel, O. Aiboudi, V. Grigorescu, Z. Ling, T. Marszalek, P. W. M. Blom, C. Ramanan, F. Lissel and U. Kraft, *Advanced Electronic Materials*, 2024, DOI: https://doi.org/10.1002/aelm.202400455, 2400455.
- 33. M. A. Rampi, O. J. A. Schueller and G. M. Whitesides, Applied Physics Letters, 1998, 72, 1781-1783.
- 34. H. Jin, J. Tian, S. Wang, T. Tan, Y. Xiao and X. Li, RSC Advances, 2014, 4, 16839-16848.
- 35. H. Torres-Pierna, C. Roscini, A. Vlasceanu, S. L. Broman, M. Jevric, M. Cacciarini and M. B. Nielsen, *Dyes and Pigments*, 2017, **145**, 359-364.
- 36. X. Li, Y. Wang, T. Matsuura and J. Meng, *Molecular Crystals and Liquid Crystals Science and Technology. Section A. Molecular Crystals and Liquid Crystals*, 2000, **344**, 301-306.
- 37. T. Yoshida and A. Morinaka, *Journal of Photochemistry and Photobiology A: Chemistry*, 1992, **63**, 227-234.
- 38. A. Radu, R. Byrne, N. Alhashimy, M. Fusaro, S. Scarmagnani and D. Diamond, *Journal of Photochemistry and Photobiology A: Chemistry*, 2009, **206**, 109-115.
- 39. R. Matsushima, M. Nishiyama and M. Doi, *Journal of Photochemistry and Photobiology A: Chemistry*, 2001, **139**, 63-69.
- 40. S. Abe, Y. Nishimura, I. Yamazaki and N. Ohta, *Chemistry Letters*, 1999, **28**, 165-166.
- 41. Q. Shen, L. Wang, S. Liu, Y. Cao, L. Gan, X. Guo, M. L. Steigerwald, Z. Shuai, Z. Liu and C. Nuckolls, *Advanced Materials*, 2010, **22**, 3282-3287.
- 42. K. E. Lee, J. U. Lee, D. G. Seong, M.-K. Um and W. Lee, *The Journal of Physical Chemistry C*, 2016, **120**, 23172-23179.

- 43. P. Lutsyk, K. Janus, J. Sworakowski, G. Generali, R. Capelli and M. Muccini, *The Journal of Physical Chemistry C*, 2011, **115**, 3106-3114.
- 44. M. Brohmann, S. Wieland, S. Angstenberger, N. J. Herrmann, J. Lüttgens, D. Fazzi and J. Zaumseil, *ACS Applied Materials & Interfaces*, 2020, **12**, 28392-28403.
- 45. M. Aghamohammadi, R. Rödel, U. Zschieschang, C. Ocal, H. Boschker, R. T. Weitz, E. Barrena and H. Klauk, *ACS Applied Materials & Interfaces*, 2015, **7**, 22775-22785.
- 46. L. Gobbi, P. Seiler, F. Diederich, V. Gramlich, C. Boudon, J.-P. Gisselbrecht and M. Gross, *Helvetica Chimica Acta*, 2001, **84**, 743-777.
- 47. K. P. Pernstich, S. Haas, D. Oberhoff, C. Goldmann, D. J. Gundlach, B. Batlogg, A. N. Rashid and G. Schitter, *Journal of Applied Physics*, 2004, **96**, 6431-6438.
- 48. S. Kobayashi, T. Nishikawa, T. Takenobu, S. Mori, T. Shimoda, T. Mitani, H. Shimotani, N. Yoshimoto, S. Ogawa and Y. Iwasa, *Nature Materials*, 2004, **3**, 317-322.
- 49. U. Zschieschang, F. Ante, M. Schlörholz, M. Schmidt, K. Kern and H. Klauk, *Advanced Materials*, 2010, **22**, 4489-4493.
- 50. S. H. Yu, S. Z. Hassan, C. So, M. Kang and D. S. Chung, *Advanced Materials*, 2023, **35**, 2203401.

Reversible switching through irradiation of capacitors and organic transistors confined employing dielectrics blended with non-ionic molecular photoswitches

The data supporting this article are shown in the ESI.

Furthermore, the raw data will be made accessible through Edmont after publication of the manuscript.